SIMULATION OF THE BASE-ISOLATED CRUAS NUCLEAR POWER PLANT IN THE M_W4.9 LE-TEIL EARTHQUAKE

Yuchuan Tang[1], Wei Zhang[2], Simin Zhang[2], Zongchao Li[3], Zhiwei Ji[4], Xiangyu Liu[5], Mao Chen[6]

[1]Associate Professor, Southeast University, Nanjing, China (ytang@seu.edu.cn)
[2]Graduate Student, Southeast University, Nanjing, China
[3]Researcher, Institute of Geophysical, China Earthquake Administration, Beijing, China
[4]Assistant Researcher, Institute of Forecasting, China Earthquake Administration, Beijing, China
[5]Researcher, State Nuclear Electric Power Planning Design & Research Institute Co., Ltd, Beijing, China
[6]VP, State Nuclear Electric Power Planning Design & Research Institute Co., Ltd, Beijing, China

ABSTRACT Seismic risk is always a severe challenge for the nuclear industry given the historical earthquake experiences as well as the growing number of nuclear power plants (NPPs) around the world. As a proven technology to reduce the horizontal seismic response of structures, base isolation has attracted interest but also arisen concern in the nuclear industry. New designs of nuclear facilities are willing to accept this type of technology for both seismic safety and economic competitiveness. However, the lack of test by actual earthquake and test of time remains an open issue on base-isolated NPPs. On November 11, 2019, the base-isolated Cruas NPP in southeast France was shaken by the M_W4.9 Le-Teil earthquake. The accelerograms recorded at the Cruas site as well as the post-earthquake inspections provide rare information to improve the scientific and engineering knowledge on the seismically isolated nuclear facilities. To this end, an international benchmark called SMATCH was launched to assess the adequacy and efficiency of current scientific and engineering practices for predicting the ground motion in the case of the Le-Teil seismic scenario and the seismic response of the base-isolated Cruas NPP. As a team participating the benchmark, the authors present ground motion and structure response simulations and results in this article.

INTRODUCTION

Seismic risk is always a severe challenge for the nuclear industry given the historical earthquake experiences as well as the growing number of nuclear power plants (NPPs) around the world. There have been at least 5 seismic events that directly affected NPPs in this century. Quite a few events (e.g., the 2007 M6.6 Niigataken Chuetsu-oki, the 2011 M9.1 Tohoku, and the 2024 M7.5 Noto Peninsula earthquakes) caused geotechnical/structural damages, equipment malfunctions, or even radiation disaster to Japanese NPPs (IAEA, 2008; Grant et al., 2016). The 2011 M5.8 Mineral earthquake triggered Units 1 & 2 at the North Anna NPP in the U.S. to shut down automatically, and the recorded motion on site exceeded the Design Basis Earthquake level (USNRC, 2011; Bhargava & Hardy, 2015). The epicenter of the 2016 M5.4 Gyeongju earthquake is only 27 km away from the Wolsong NPP in South Korea, which revealed the importance of high-frequency (> 10 Hz) content for the Korean NPPs (Gupta et al., 2019). More than 30 countries have endorsed the declaration to triple the global nuclear energy by 2050 during the United Nations Climate Change Conferences, COP28 and COP29. More and more countries located in earthquake-prone regions are taking the initiative to build NPPs.

As a proven technology to reduce the horizontal seismic response of structures, base isolation has attracted interest from the nuclear industry for long. Pioneering application of seismic isolation system to NPPs happened in France in late 1970s (Moussallam et al., 2013). A total of 3624 polychloroprene laminated rubber bearings, which was invented by Eugène Freyssinet, are installed in the four-unit Cruas NPP to isolate the base of the building structures from the lower raft foundation (Labbé, 2013). Similar seismic isolation systems have been implemented in four other nuclear facilities in France and the Koeberg NPP in South Africa. Following the seismic damages to the Kashiwazaki-Kariwa NPP in 2007 and to the

Fukushima Daiichi NPP in 2011, there is a global renewal of research interest in seismic isolation for NPPs. Both the U.S. Nuclear Regulatory Commission (USNRC) and the U.S. Department of Energy funded studies on the seismic isolation of nuclear facilities between 2008 and 2018 (Whittaker et al., 2018). These researches provided technical underpinnings for the newly added chapters on building-level seismic isolation for nuclear facilities in the ASCE/SEI 4-16 (ASCE, 2017) and ASCE/SEI 43-19 (ASCE, 2021) codes as well as for three contractor reports, NUREG/CR-7253 (Kammerer et al., 2019), NUREG/CR-7254 (Kumar et al., 2019a), and NUREG/CR-7255 (Kumar et al., 2019b). The International Atomic Energy Agency published the IAEA-TECDOC-1905 document to elaborate the technical basis for the use of seismic isolation systems in nuclear installations (IAEA, 2020). Hou and Dong (2022) introduced the researches in this field in East Asian countries. Liu et al. (2024) proposed a hybrid system that combines three-dimensional base isolation and geotechnical seismic isolation for NPP buildings. Parsi et al. (2022) demonstrated a pathway to standardized designs for advanced reactors through using seismic isolation. Early this year, Southern Company (2025) submitted to USNRC the guidelines for implementing seismic base isolation in advanced nuclear reactors. Additionally, various innovative seismic isolation systems have been proposed for small modular reactors (Mori et al., 2023; Kumawat et al., 2024).

The engineering application of seismic isolation to nuclear island buildings is still limited mainly due to the concerns about the displacement control, the long-term performance, and the horizontal–vertical interaction of the isolation system. Base isolation technology for NPPs is still challenged by international community given the lack of realistic tests on such facilities by actual earthquakes. This kind of rare event that a seismically isolated NPP being subjected to a real earthquake did happen in France on November 11, 2019. The Le-Teil earthquake, a M_w4.9 event, shook the base-isolated Cruas NPP at an epicentral distance around 15 km, triggering alarm in the main control room and leading to shutdown of the operating reactors. The site contains two pairs of twined French CP2 standardized plants, each has a pressurized water reactor of 900 MWe. When the seismic waves reached the Cruas NPP site, the ground and in-structure responses were recorded in accordance with the operational procedures. Moreover, post-earthquake inspections and walkdowns were performed to collect in-situ data on various Structures, Systems and Components (SSCs). The recordings as well as the post-earthquake inspections provide rare information to improve the scientific and engineering knowledge on the seismically isolated nuclear facilities.

In this context, Institut de Radioprotection et de Sûreté Nucléaire (IRSN) and Électricité de France (EDF), under the aegis of the OECD Nuclear Energy Agency (NEA), launched an international benchmark called SMATCH in 2022. The SMATCH benchmark takes advantage of the occurrence of the Le-Teil earthquake and the recorded data at the Cruas NPP to assess the adequacy and efficiency of current scientific and engineering practices for predicting (1) the ground motion in the case of the Le-Teil seismic scenario and (2) the seismic response of base-isolated NPP buildings. The benchmark consists of four phases: Phase 1 – Kick-off, Phase 2 – Seismic ground motion characterization for the Cruas site, Phase 3 – Seismic response simulation of the base-isolated Cruas NPP, and Phase 4 – Concluding.

The authors, from three institutes, form a team to participate the SMATCH benchmark. In the first phase of the benchmark, we mainly adopted the empirical Green's function method to simulate ground motion at the Cruas NPP site, relying on the high-density seismic monitoring network in France to provide data support for the Green's function. The synthetic acceleration waveforms show similarity to the recorded accelerograms at the RAN station at the Cruas site. The synthesized ground motions, in comparison with the RAN recording, are used as input to the structural analysis of the base-isolated plant buildings in Phase 3 of the benchmark. This article presents our study in the SMATCH benchmark. Following a brief introduction on the Le-Teil earthquake event and the ground motion simulation, we elaborate on the structural modelling, the dynamic analysis, and the comparison of our results with the recorded seismic response of the Cruas plant buildings. The effect of seismic isolation is also investigated by comparing the base-isolated structural response to the simulated fixed-base structural response under the same ground motion excitation.

SEISMIC EVENT AND OBSERVATION

On November 11, 2019, a M_W4.9 (M_S4.5) event, referred to as the Le-Teil earthquake, occurred in the Ardèche region in Le Teil municipality at approximately 10 km to the west of the city Montélimar in France, a moderate seismicity area. The ground motion lasted several seconds in the vicinity of the epicenter and was felt by the population in the southeast of France. The unexpected level of damage (epicentral intensity VIII according to Sira et al. (2020)) for this magnitude attests an intense ground shaking. The earthquake causative fault, which was not considered as active, is part of the Cévennes fault system (Ritz et al., 2020). Seismological, geodetical and field observations indicate a reverse-fault mechanism, a rupture area of about 4 km by 1.5 km, a hypocentral depth about 1 km and surface rupture evidences (Cornou et al., 2021). Such a shallow depth is exceptional for moderate-sized earthquakes occurring in stable continental regions (Causse et al., 2021). The shallow location may be related to quarry extraction directly above the rupture area (De Novellis et al., 2020).

The Le-Teil earthquake occurred within the lower Rhône river valley, an industrial region hosts several operating nuclear facilities. None of the reference earthquake spectra for the design basis of the facilities were exceeded (Bitar et al., 2022). Each facility is equipped with a seismic safety monitoring system, in Unit 1, called the EAU system to provide alarm in the control rooms in case of earthquakes. The EAU system at the Cruas NPP consists of four triaxial accelerometers (i.e., sensors) installed at the following locations:

- EAU 001 MV sensor on the bottom floor at Elev. −3.50 m in the Unit 1 Reactor Building,
- EAU 002 MV sensor on the floor at Elev. +20.00 m in the Unit 1 Reactor Building,
- EAU 003 MV sensor on the floor at Elev. ±0.00 m in the Auxiliary Building,
- EAU 004 MV sensor on a small concrete footing at ground level in free field (away from heavy buildings).

Every sensor is installed in such a way that its three orthogonal axes coincide with the principal axes of the buildings. Exceeding the threshold of 0.01g on one of the 3 axes of any one sensor will activate the recording of all the sensors and trigger a Category-2 alarm in all the control rooms at the plant site. This recording threshold was exceeded under the 2019 Le-Teil earthquake. The three sensors installed in the Cruas plant buildings (i.e., EAU 001, 002, and 003) recorded accelerograms during the Le-Teil earthquake. In addition, tri-axial free-field ground acceleration was recorded at the RAN station (44.636253° N, 4.758796° E) at the Cruas site. The recording at RAN will be used to verify the subsequent ground motion simulation and used as seismic input in the structure response simulation later in this study. The recordings at the EAU sensors will be used as benchmark to verify our simulated structure response. All the recordings are provided by the SMATCH committee to the benchmark participants.

SIMULATION OF GROUND MOTION

The authors take a physics-based approach to simulate ground motions at the Cruas site coherently with the 2019 Le-Teil earthquake characteristics. The seismic source model used in this work is a combination of the finite fault source model and the Asperity–Characteristic source model. In addition to the basic source parameters provided by the SMATCH committee, a thorough literature review is conducted to collect the crustal velocity structure at the epicenter, the initial rupture position of the source, the rise time of small earthquakes, the proportion relationship between shear wave velocity and rupture velocity, and parameters related to asperity. Various uncertainties of the model parameters (e.g., focal mechanism, rupture velocity, initial rupture point, asperity parameters) are fully considered in the subsequent calculation process.

The empirical Green's function method (Li et al., 2022; Li et al., 2025) is adopted for ground motion simulation. Firstly, we select appropriate small earthquake events (the acceleration waveforms of the small earthquakes) as Green's function. From the earthquake catalogue in southeast France, two small earthquake waveforms with a magnitude of M_L2.2, which occurred at (4.64579°E, 44.5637°N) on November 13, 2019 and at (4.65436°E, 44.5489°N) on November 23, 2019 respectively, are selected as the Green's function. These two small earthquakes satisfy a propagation path and site environment similar to the Le-Teil event. In the second step, the three components of the selected small earthquakes are pre-processed such that each component is intercepted from a data segment at 30 seconds after the initial motion of the P-wave. Then the processed components are taken as Green's functions input to the computer program of the empirical Green's function method. Afterwards, we arrange and combine multiple source parameters to obtain source models for various possible scenarios, and further combine them with the selected small earthquake waveforms to synthesize ground motion results for different scenarios. Finally, we combine the spatial distribution characteristics of ground motion, rapid estimation of seismic intensity, and Shake-Map provided by multiple research institutes (e.g., the United States Geological Survey, European Earthquake Data Center, French Earthquake Data Center) to verify the rationality and reliability of ground motion simulation results from multiple perspectives.

Our ground motion simulation results are compared with the recorded accelerograms at RAN in Figure 1. Seven equally possible random scenarios are presented in the figure from top to bottom. The left, middle, and right columns show the EW, NS, and UD components of the acceleration, respectively. The simulation results exhibit similarity with the observation. The simulated ground acceleration scenarios will be used as alternative seismic input for the structure response analysis in the next section.

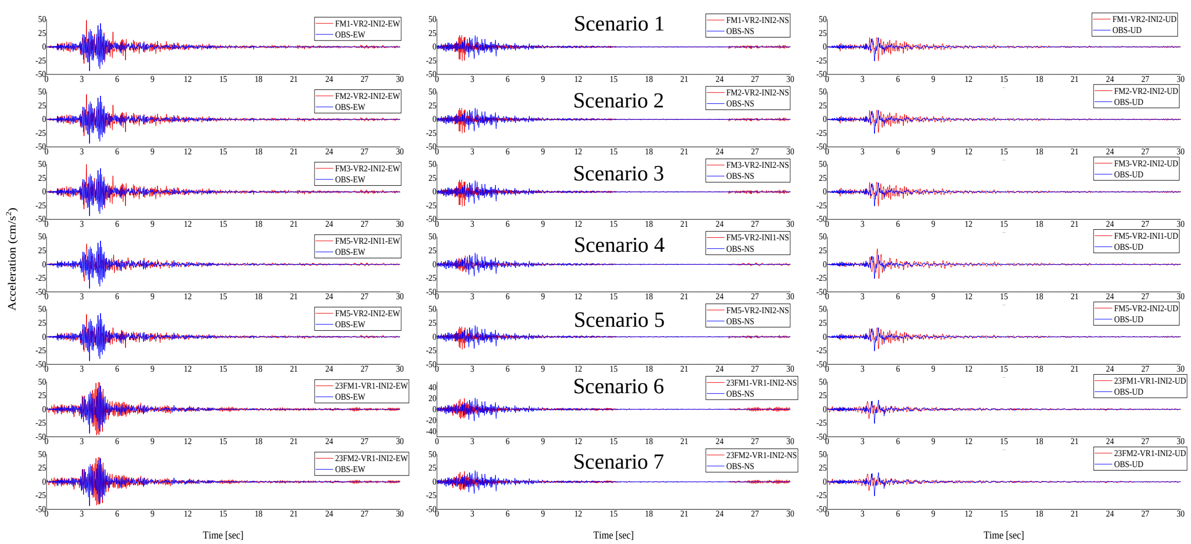

Figure 1. Comparison between simulated waveform (in red) and observed waveform (in blue).

SIMULATION OF STRUCTURE RESPONSE

Finite Element Model of Nuclear Island

The SMATCH committee provided guidelines and data for modelling the Cruas structural response to the Le-Teil earthquake. A finite element mesh of the Nuclear Island (NI) buildings of Units 1 & 2 at the Cruas site is given in a universal extension (".unv") file. Complementary information including element features, material properties, and constraints are given in a text file. Based on these two files, the authors made effort to build a finite element model of the base-isolated NI buildings in the open-source numerical simulation platform, Salome-Meca. As shown in Figure 2, the Unit 1 Reactor Building and the Auxiliary Building are modelled in detail with Discrete Kirchhoff plate (DKT) elements being used for the containment shell, the internal structure, the shear walls, and the floor slabs. Three-dimensional Timoshenko beam (POU_D_T) elements are used to model the beams and columns in the Auxiliary Building. In addition, seven other building structures in the NI are each modelled as a lumped-mass stick with POU_D_T beam elements, discrete (DIS_T or DIS_TR) elements as well as multi-point constraints (LIAISON_SOLIDE). The base slabs of the nine buildings are connected together to form a raft, which is called the upper raft to be distinguished from the raft foundation of the NI (i.e., the lower raft). Between the upper and the lower rafts exist the seismic isolation system. In the isolation system, 1812 laminated elastomeric bearings are installed on top of 401 reinforced concrete pedestals, each pedestal receiving 2, 4, or 8 bearings according to its horizontal dimension. The layout of the pedestals of different dimensions in the model are depicted in Figure 3 along with a photo showing them in the construction stage. The pedestals are modelled with the POU_D_T elements, while the bearings are modelled with the DIS_TR elements. Each bearing, 500 mm square in plan, is composed of seven layers in thickness — four steel layers and three polychloroprene layers alternating. The three elastomer layers have identical thickness of 13.5 mm, and the total thickness of the bearing is 66.5 mm. The dynamic shear modulus of the elastomer is estimated to be 1.53E6 N/m^2 based on its original value of 1.10E6 N/m^2 and the aging factor provided by the SMATCH committee. It is known that the horizontal stiffness of a laminated bearing varies drastically with the vertical pressure (Labbé, 2013). However, it is unclear under what pressure level the original value of the shear modulus was obtained. In addition, the vertical pressure on the bearings may vary under three-dimensional earthquake excitation. Given these uncertainties, the authors introduce a modification factor to tune the horizontal stiffness of the bearing such that the simulation result can approach the observation under the Le-Teil earthquake. For each bearing, the damping coefficient associated with the horizontal stiffness k is computed as $2\xi k/\omega$, where the damping ratio $\xi \approx 7\%$ based on the SMATCH data and the circular frequency ω takes the average of the dominant modal frequencies of the isolated NI as discussed later. The elastic modulus of the concrete material varies from 3.29E10 N/m^2 at the lower raft to 3.36E10 N/m^2 at the Auxiliary Building and to 3.70E10 N/m^2 at the containment shell. A Rayleigh damping toward 5% is implemented to the structures above the isolation system.

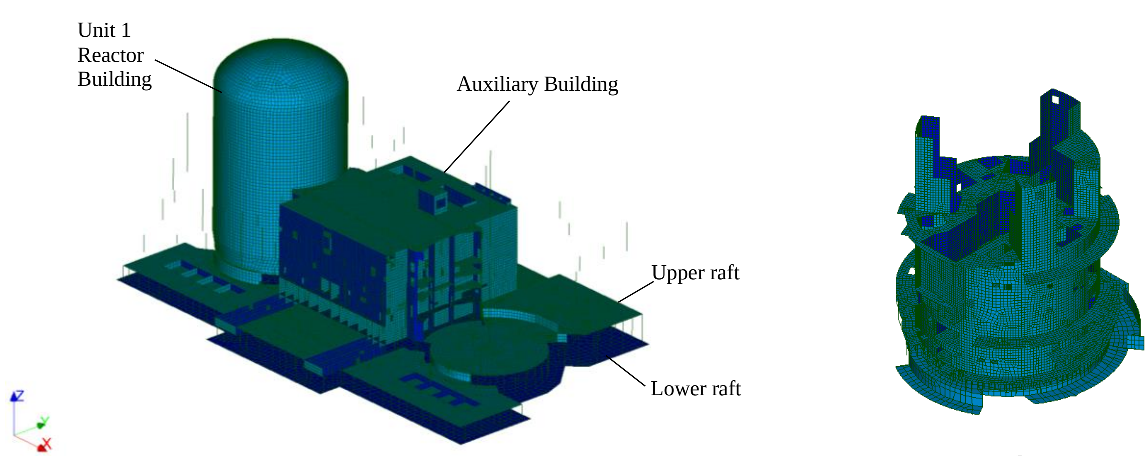

(a) (b)

Figure 2. Finite element model of NI: (a) perspective, (b) internal structure of Reactor Building.

Modal Analyses and Comparison

Modal analysis of the NI is conducted using the Code-Aster finite element analysis software embedded in the Salome-Meca platform. Two cases of boundary constraint are considered separately. In the first case, only the lower raft is constrained to model the actual base-isolated NI. In contrast, the second case has both the lower and the upper rafts constrained to resemble a hypothetical fixed-base situation. The frequencies and the mass participation ratios of the principal modes of the base-isolated NI resulted from this study are compared with the benchmark given by the SMATCH committee in Table 1. Our model is able to capture the major modes around 1.5 Hz when the bearing stiffness modification factor equals 2, which is thus used throughout this study. The comparison between the base-isolated and the fixed-base cases in Table 1 shows that the isolation system lowers the dominant frequency of the NI to be one-third, i.e., elongating the period by three times.

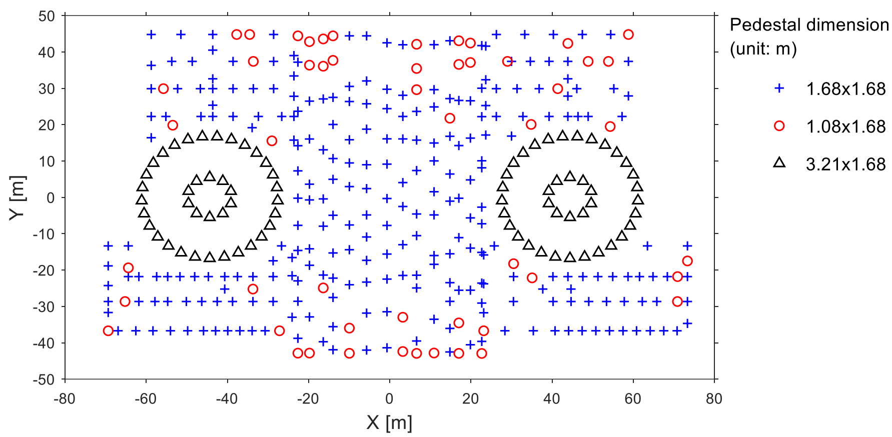

(Photo courtesy of SMATCH committee)

Figure 3. Layout of pedestals for base isolation bearings.

Table 1: Principal natural vibration modes.

	Mode #	Frequency [Hz]	Mass participation ratio in X	Mass participation ratio in Y
SMATCH benchmark – base isolated	9	1.48	42.5%	0.49%
	10	1.49	0.54%	88.1%
	11	1.51	45.6%	0.12%
This study – base isolated	1	0.74	0.05%	7.50%
	2	1.44	59.04%	26.48%
	3	1.46	28.58%	36.29%
	4	1.58	0.73%	8.86%
	5	1.61	1.03%	9.79%
This study – fixed base	2	3.69	6.22%	5.82%
	3	4.21	4.30%	4.75%
	4	4.22	2.26%	6.34%
	5	4.36	6.21%	2.06%
	6	5.01	24.22%	0.01%
	9	6.82	0.03%	2.68%
	16	7.49	0.01%	3.86%

Seismic Analyses and Comparison

At first, two seismic simulations are performed on the finite element model of the NI with the base-isolation condition using Code-Aster. In Simulation 1, the tri-axial Le-Teil ground motion recorded at the RAN station is used as seismic input. In contrast, Simulation 2 takes one of the synthetic ground motion scenarios shown in Figure 1 as input. In both simulations, the original ground motion components in NS and EW have been converted to be in the X and Y directions (see Figure 2a). For sake of brevity, only the result from Simulation 2 with Scenario 1 as input is presented hereafter. In-structure responses at the locations of the EAU sensors are obtained from dynamic analysis of the finite element model in time domain, using implicit Newmark-β time integration scheme. Acceleration time series of the in-structure responses from Simulations 1 and 2 are compared in Figure 4 with the actual recordings provided by the SMATCH committee along the local u, v, w axes, which correspond to −Y, X, and Z directions in Figure 2a. The result from Simulation 1 approaches the recorded response reasonably well, although underpredicting the acceleration peaks at EAU 002 by 40%–50%. The 5%-damped response spectra of these in-structure motions at EAU 002, located at Elev. +20.0 m in the Reactor Building internal structure, are computed and compared in Figure 5. The result from Simulation 1 captures the first peak around 1.5 Hz in the horizontal in-structure response spectra (ISRS), while it fails to resemble the high-frequency content in the actual response at EAU 002. The horizontal ISRS associated with Simulation 2 generally show much lower amplitude, which should be mainly attributed to the weakness of the simulated ground motion. The ISRS are more comparable in the vertical direction, which is supposed not to be affected by the horizontal isolation system. In the base-isolated simulations, the relative displacement between the upper raft and the lower raft have been monitored throughout. The shift in either horizontal direction does not exceed 2 mm.

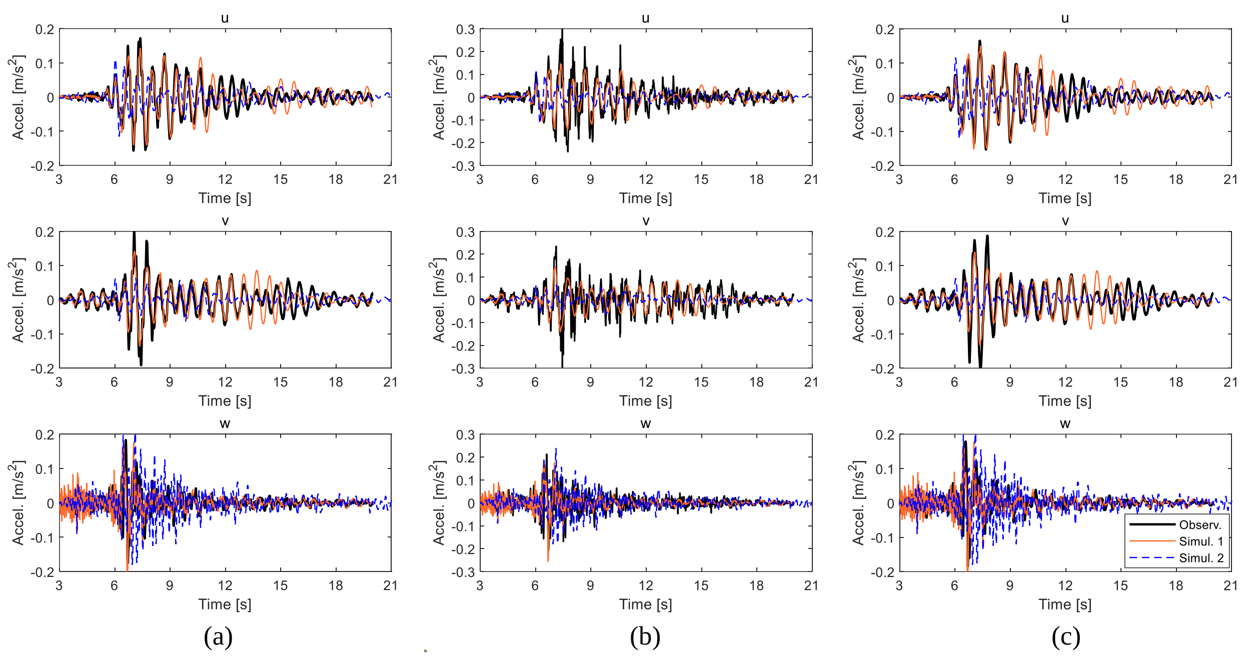

Figure 4. In-structure response of base-isolated NI at: (a) EAU 001, (b) EAU 002, (c) EAU 003.

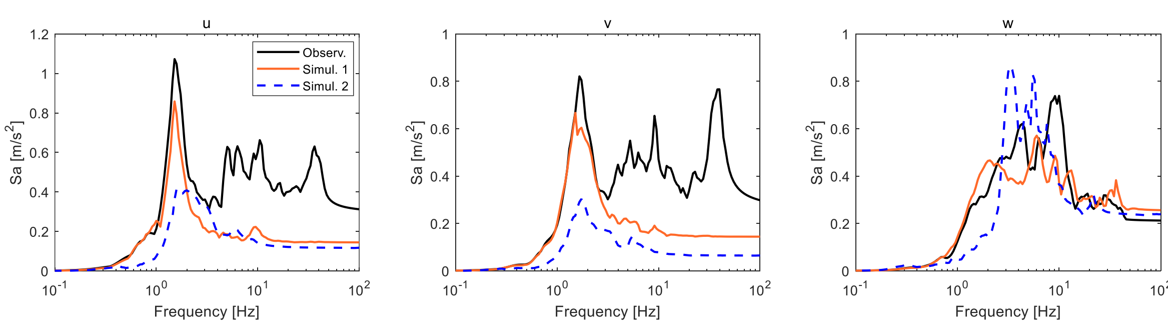

Figure 5. Comparison of ISRS at EAU 002 for base-isolated case.

Next, a simulation of the hypothetical fixed-base NI model subjected to the recorded ground motion at the RAN station is performed. The resulted in-structure responses at the locations of the EAU sensors are compared with the actual observations by the sensors in the base-isolated NI to investigate the effect of seismic isolation. As shown in Figure 6, the seismic isolation tends to mitigate the horizontal in-structure response and filter out high-frequency content. The effect of the isolation is further demonstrated by comparing the ISRS in Figure 7. The vertical responses of the isolated and the fixed-base cases are alike since the horizontal isolation system at the Cruas NPP has minimal impact in the vertical.

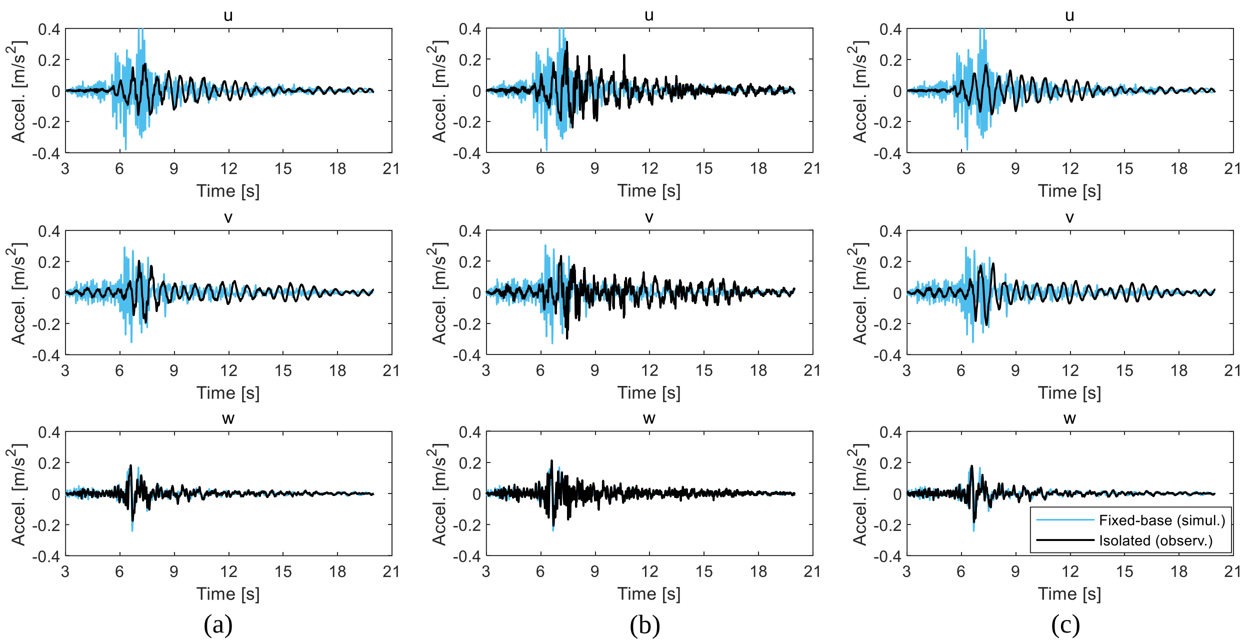

Figure 6. Base-isolated response versus fixed-base response at (a) EAU 001, (b) EAU 002, (c) EAU 003.

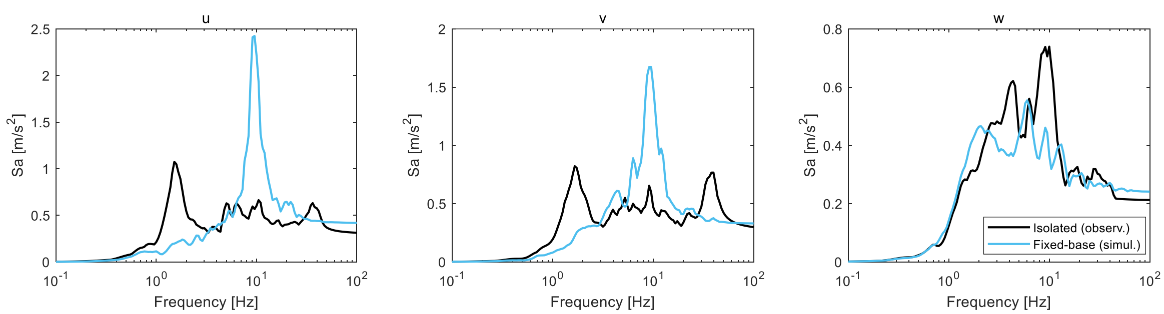

Figure 7. Comparison of ISRS at EAU 002 between base-isolated case and fixed-base case.

CONCLUSION

Participating the SMATCH international benchmark organized by IRSN and EDF, the authors carried out a comprehensive study on the ground motion simulation in the case of the 2019 M_W4.9 Le-Teil seismic scenario as well as on the seismic response of the base-isolated nuclear island of the Cruas Units 1 & 2 in France. The empirical Green's function method is employed for the physics-based ground motion simulation. A combination of the finite fault source model and the Asperity–Characteristic source model is adopted with due consideration for various uncertainties in the model parameters. The simulated ground motion scenarios at the Cruas site resemble the waveform of the accelerogram recorded during the 2019

Le-Teil event. The simulated scenarios, however, are later found out inadequate to cause as large in-structure response as the actual earthquake did. The in-structure seismic response of the Cruas plant buildings are obtained from sophisticated finite element modelling of the nuclear island structures with the base isolation system. The finite element model is able to capture the principal natural vibration modes around 1.5 Hz as well as yield in-structure response close to the actual observation recorded by the EAU accelerometers. By comparing the simulated fixed-base response to the actual base-isolated recordings, the effect of seismic isolation on the horizontal response is evident in terms of both amplitude alleviation and high-frequency filtering. In addition, the simulations show small horizontal displacement (< 2 mm) at the isolation system under the Le-Teil excitation.

Following this benchmark, we would continue to investigate several issues for improvement. The first is the underneath difference between the simulated ground motion and the actual recording regarding their dissimilar consequences on the building structural response. The second issue is that the empirical tuning on the elastomeric bearing stiffness needs theoretical and experimental validation. Moreover, the high-frequency (> 4 Hz) peaks missing in the base-isolated ISRS from our simulation indicates the possibility that the current way of modelling the bearings may overly filter out the high-frequency content in the seismic input. A clue may exist in Figure 7 where the secondary peaks around 10 Hz in the base-isolated horizontal ISRS coincide with the global peak of the fixed-base ISRS.

REFERENCES

American Society of Civil Engineers (ASCE). (2017). *Seismic Analysis of Safety-related Nuclear Structures and Commentary (ASCE/SEI 4-16)*. Reston, VA, U.S.

American Society of Civil Engineers (ASCE). (2021). *Seismic Design Criteria for Structures, Systems, and Components in Nuclear Facilities (ASCE/SEI 43-19)*. Reston, VA, U.S.

Bhargava, D. and Hardy, G. (2015). "North Anna nuclear power station long term seismic safety: from Mw 5.8 Mineral Virginia earthquake of 2011 to probabilistic risk assessment," *23rd International Conference on Structural Mechanics in Reactor Technology* (*SMiRT-23*), Manchester, U.K., Division VII, Paper ID 822.

Bitar, I., Viallet, E., Lancieri, M. et al. (2022). "CRUAS 2019 international benchmark on a seismic base isolated NPP which experienced a real earthquake," *26th International Conference on Structural Mechanics in Reactor Technology* (*SMiRT-26*), Berlin/Potsdam, Germany.

Causse, M., Cornou, C., Maufroy, E. et al. (2021). "Exceptional ground motion during the shallow Mw 4.9 2019 Le Teil earthquake, France," *Communications Earth & Environment*, 2, 14.

Cornou, C., Ampuero, J.-P., Aubert, C. et al. (2021). "Rapid response to the Mw 4.9 earthquake of November 11, 2019 in Le Teil, Lower Rhône Valley," *Comptes Rendus Geoscience*, 353(S1) 441–463.

De Novellis, V., Convertito, V., Valkaniotis, S. et al. (2020). "Coincident locations of rupture nucleation during the 2019 Le Teil earthquake, France and maximum stress change from local cement quarrying," *Communications Earth & Environment*, 1, 20.

Grant, F. F., Tang, Y., Hardy, G. S. and Kassawara, R. (2017). "Seismic damage indicating parameters at nuclear power plants affected by the 2011 Tohoku-Oki earthquake and plant shutdown criteria," *Earthquake Spectra*, 33(1) 109–121.

Gupta, A., Cho, S.-G., Hong, K.-J. and Han, M. (2019). "Current state of in-cabinet response spectra for seismic qualification of equipment in nuclear power plants," *Nuclear Engineering and Design*, 343 269–275.

Hou, N. and Dong, J. (2022) "Development and expectation of seismic isolation of nuclear power plant structure," *26th International Conference on Structural Mechanics in Reactor Technology* (*SMiRT-26*), Berlin/Potsdam, Germany.

International Atomic Energy Agency (IAEA). (2008). *Follow-up IAEA Mission in Relation to the Findings and Lessons Learned from the 16 July 2007 Earthquake at Kashiwazaki-Kariwa NPP*, Volumes I & II. Vienna, Austria.

International Atomic Energy Agency (IAEA). (2020). *Seismic Isolation Systems for Nuclear Installations (IAEA-TECDOC-1905)*. Vienna, Austria.

Kammerer, A. M., Whittaker, A. S., Constantinou, M. C. (2019). *Technical Considerations for Seismic Isolation of Nuclear Facilities (NUREG/CR-7253)*. United States Nuclear Regulatory Commission, Washington, D.C., U.S.

Kumar, M., Whittaker, A. S., Constantinou, M. C. (2019a). *Seismic Isolation of Nuclear Power Plants Using Sliding Bearings (NUREG/CR-7254)*. United States Nuclear Regulatory Commission, Washington, D.C., U.S.

Kumar, M., Whittaker, A. S., Constantinou, M. C. (2019b). *Seismic Isolation of Nuclear Power Plants Using Elastomeric Bearings (NUREG/CR-7255)*. United States Nuclear Regulatory Commission, Washington, D.C., U.S.

Kumawat, S. R., Kumar, M. and Laskar, A. (2024). "Three-dimensional seismic isolation of small modular reactors using metamaterials and elastomeric bearings," *27th International Conference on Structural Mechanics in Reactor Technology* (*SMiRT-27*), Division X, Yokohama, Japan.

Labbé, P. (2013). "EDF experience on design and construction of nuclear power plants on seismic isolation systems," *International Conference on Technical Innovation in Nuclear Civil Engineering* (*TINCE 2013*), Paris, France.

Li, Z., Sun, J., Gao, M. et al. (2022). "Evaluation of horizontal ground motion waveforms at Sedongpu Glacier during the 2017 M6.9 Mainling earthquake based on the equivalent Green's function," *Engineering Geology*, 306, 106743.

Li, Z., Ji, Z., Sun, J. et al. (2025). "High-probability ground motion simulation in Maduo County for the Maduo M_S7.4 earthquake in 2021: A possible supershear earthquake," *J. Earth Sci.*, 36 781–800.

Liu, Y., Li, J. and Lin, G. (2024). "Seismic mitigation analysis of three-dimensional base-isolated nuclear structures with soil-dependent isolation system under extreme earthquakes," *Engineering Structures*, 311, 118187.

Mori, T., Shimada, T., Kai, S. et al. (2023). "Experiment of floating seismic isolation system for SMR," *Proceedings of the 30th International Conference on Nuclear Engineering (ICONE30)*, Kyoto, Japan.

Moussallam, N., Allain, F., Petre-Lazar, I. et al. (2013). "Seismic isolation of nuclear structures – Overview of the French practice and experience," *22nd International Conference on Structural Mechanics in Reactor Technology* (*SMiRT-22*), San Francisco, U.S., Division VI.

Parsi, S. S., Lal, K. M., Kosbab, B. D., et al. (2022). "Seismic isolation: A pathway to standardized advanced nuclear reactors," *Nuclear Engineering and Design*, 387, 111445.

Ritz, J. F., Baize, S., Ferry, M. et al. (2020). "Surface rupture and shallow fault reactivation during the 2019 Mw 4.9 Le Teil earthquake, France," *Communications Earth & Environment*, 1, 10.

Sira, C., Schlupp, A., Bertrand, E. et al. (2020). *Rapport macrosismique n°4, Séisme du Teil (Ardèche) 11 novembre 2019 à 11 h 52 locale, Magnitude 5,2 ML (RENASS), Intensité communale max VII-VIII (EMS98)*, Report BCSF-RENASS-2020-R2, University of Strasbourg, France.

Southern Nuclear Development, LLC. (2025). *Guidelines for Implementing Seismic Base Isolation in Advanced Nuclear Reactors (SC-SND8932-001)*. Atlanta, GA, U.S.

U.S. Nuclear Regulatory Commission (USNRC). (2011). *Technical Evaluation Related to Plant Restart After the Occurrence of an Earthquake Exceeding the Level of the Operating Basis and Design Basis Earthquakes*, Washington, D.C., U.S.

Whittaker, A. S., Sollogoub, P. and Kim, M. K. (2018). "Seismic isolation of nuclear power plants: Past, present and future," *Nuclear Engineering and Design*, 338 290–299.